Base Control of Electron-Transfer Reactions of Manganese(III) Porphyrins

Ikuo Nakanishi,[a] Shunichi Fukuzumi,*[a] Jean-Michel Barbe,[b] Roger Guilard,*[b] and Karl M. Kadish*[c]

Keywords: Electron transfer / Kinetics / Manganese / Metalloporphyrins / Quinones

Homogeneous electron-transfer kinetics for the reduction of four different manganese(III) porphyrins using different reductants were examined in deaerated acetonitrile, and the resulting data were evaluated in light of the Marcus theory of electron transfer to determine electron-exchange rate constants between manganese(III) and manganese(II) porphyrins. The investigated compounds are represented as (P)MnCl, where P = the dianion of dodecaphenylporphyrin (DPPX; X = H_{20}, $Cl_{12}H_8$, or F_{20}) or tetraphenylporphyrin (TPP). The electron transfer from semiquinone radical anion derivatives to $(P)Mn^{III}Cl$ leads to formation of the corresponding Mn^{II} complex, $[(P)Mn^{II}Cl]^-$. The electron-exchange rate constants derived from the electron-transfer rate constants decrease with an increasing degree of nonplanarity of the porphyrin macrocycle and follow the order: (TPP)MnCl (3.1×10^3 $M^{-1}\cdot s^{-1}$) > ($DPPH_{20}$)MnCl (1.1×10^{-2} $M^{-1}\cdot s^{-1}$) > ($DPPCl_{12}H_8$)MnCl (3.5×10^{-4} $M^{-1}\cdot s^{-1}$) > ($DPPF_{20}$)MnCl (4.3×10^{-6} $M^{-1}\cdot s^{-1}$). The coordination of two molecules of pyridine (py) or DMSO to ($DPPH_{20}$)MnCl to form $[(DPPH_{20})Mn(py)_2]^+$ or $[(DPPH_{20})Mn(DMSO)_2]^+$ enhances the rate of electron-transfer reduction. This indicates that there is a significant decrease in the reorganization energy upon axial ligand coordination of pyridine or DMSO.

Introduction

Metalloporphyrins have been utilized as important electron carriers in a variety of biological and chemical redox systems, since electron-transfer reactions of metalloporphyrins can be finely tuned by the metal, the porphyrin macrocycle and the axial ligands.[1] The axial ligand has merited special attention among the factors which control the rates of electron-transfer reactions of metalloporphyrins, since the redox properties of metalloporphyrins can be finely tuned by the addition of an external base ligand. Although there seems to be no need to accelerate further the electron-transfer reactions of metalloporphyrins, which are normally fast, the rates of electron transfer of some metalloporphyrins are known to be relatively slow because of the large reorganization energy associated with the electron transfer.[1] In this context, we have recently reported that the rates of metal-centered electron-transfer oxidation of $(OETPP)Fe^{III}(R)$ (OETPP = the dianion of octaethyltetraphenylporphyrin and R = σ-bonded axial ligand such as Ph), which has a saddle-shaped nonplanar porphyrin macrocycle, are much slower than those of $(OEP)Fe^{III}(R)$ (OEP = the dianion of octaethylporphyrin), which has a planar porphyrin macrocycle, and this can be associated with the large reorganization energies upon electron-transfer oxidation of the metal center of the nonplanar porphyrins.[2] It has also been shown that the slow electron transfer of a nonplanar iron(III) porphyrin is significantly accelerated by axial coordination of pyridine due to the decreased reorganization energy upon electron-transfer oxidation.[2] Such nonplanar conformations of porphyrins have been suggested as being related to their functions in biological systems.[3−8]

We report herein the effects of conformational distortions of the porphyrin ring on the electron-transfer kinetics for reduction of (P)MnCl, where P represents either the dianion of tetraphenylporphyrin (TPP), which is planar, or the dianion of dodecaphenylporphyrins (DPPX, X = H_{20}, $Cl_{12}H_8$, F_{20}) which are known to adopt a nonplanar conformation.[3,9−11] Manganese is an essential metal in several biological systems which are involved in electron-transfer reactions,[12] and extensive efforts have therefore been devoted to elucidating electron-transfer processes in synthetic manganese porphyrins.[13−18] The detailed kinetics for the electron-transfer reduction of (P)MnCl by the semiquinone radical anion ($Q^{\bullet -}$) in Equation (1) enables us to compare the reorganization energies λ for reduction of manganese porphyrins with a planar macrocycle, as in (TPP)MnCl, and a nonplanar macrocycle, as in (DPPX)MnCl.[19] We also report the acceleration in the rate of electron-transfer reduction of ($DPPH_{20}$)MnCl upon axial coordination of pyridine or DMSO, and this data should provide valuable insights into those factors which control the electron-transfer reactivities of metalloporphyrins.

[a] Department of Material and Life Science,
Graduate School of Engineering, Osaka University, CREST,
Suita, Osaka 565−0871, Japan
Fax: (internat.) +81-6-6879−7368
E-mail: fukuzumi@ap.chem.eng.osaka-u.ac.jp
[b] LIMSAG, UMR 5633, Université de Bourgogne,
Faculté des Sciences "Gabriel",
6 Boulevard Gabriel, F-21100 Dijon, France
Fax: (internat.) +33-3-8039−6117
E-mail: roger.guilard@u-bourgogne.fr
[c] Department of Chemistry, University of Houston,
Houston TX 77204−5641, USA
Fax: (internat.) +1−713−743−2745
E-mail: kkadish@uh.edu

  1434−1948/00/0707−1557 $ 17.50+.50/0

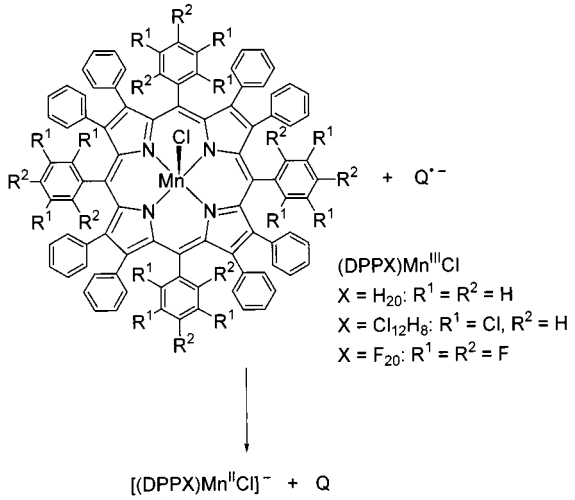

(1)

Results and Discussion

Slow Electron-Transfer Reduction of Nonplanar Manganese Porphyrins

The one-electron reduction potentials (E^0_{red}) of (P)MnCl determined by the cyclic voltammetry (CV) measurements[16] are shown in Table 1.

Table 1. Rate constants (k_{et}) and free energy changes (ΔG^0_{et}) for electron-transfer reduction of (P)MnCl with semiquinone radical anion ($Q^{\bullet -}$) in deaerated MeCN or deaerated DMSO at 298 K, their one-electron reduction potentials (E^0_{red}, V vs. SCE) and electron self-exchange rate constants (k_{ex}) of (P)MnCl/[(P)MnCl]$^-$

(P)MnCl	E^0_{red} [a] [V]	ΔG^0_{et} [eV]	k_{et} [b] [M^{-1} s^{-1}]	k_{ex} [c] [M^{-1} s^{-1}]
(TPP)MnCl	−0.22[d]	−0.28	5.4×10^7	3.1×10^3
$(DPPH_{20})$MnCl	−0.36	−0.14	1.3×10^4	1.1×10^{-2}
$(DPPH_{20})$MnCl	−0.36	−0.22[e]	4.1×10^4	6.6×10^{-3}
$[(DPPH_{20})Mn(py)_2]Cl$	−0.41	−0.09	1.9×10^6	1.5×10^3
$[(DPPH_{20})Mn(py)_2]Cl$	−0.41	−0.17[e]	5.8×10^6	8.4×10^2
$[(DPPH_{20})Mn(DMSO)_2]Cl$	−0.40	−0.10	2.3×10^6	1.6×10^3
$(DPPCl_{12}H_8)$MnCl	−0.15	−0.35	8.6×10^4	3.5×10^{-4}
$(DPPF_{20})$MnCl	0.04	−0.54	2.0×10^5	4.3×10^{-6}

[a] Determined in PhCN unless otherwise noted, 0.1 M TBAP, scan rate = 0.1 V s^{-1}. See ref.[16] The experimental error is within ±0.005 V. – [b] The experimental error is within ±5%. – [c] Determined using Equations 3–5. – [d] Determined in MeCN, 0.1 M TBAP, scan rate = 0.1 V s^{-1}. – [e] Electron-transfer reduction by methyl-*p*-benzosemiquinone radical anion ($MeQ^{\bullet -}$).

The CV measurements on (TPP)MnCl were performed in both MeCN and PhCN. The E^0_{red} value in MeCN (−0.22 V) is essentially the same as that in PhCN (−0.23 V). In spite of the electron-withdrawing effect of the additional phenyl groups in $DPPH_{20}$, the E^0_{red} value of $(DPPH_{20})$MnCl (−0.36 V) is more negative than that of (TPP)MnCl (−0.22 V). This may be ascribed to the stronger Mn^{III}–N binding of the nonplanar conformation of the $DPPH_{20}$ ligand than the planar TPP ligand. Since the E^0_{red} value of $(DPPF_{20})$MnCl remained unchanged after addition of excess Cl^- (0.1 M), there should be no dissociation of Cl^- after reduction of Mn^{III} to Mn^{II}.

Semiquinone radical anions are employed as one-electron reductants whose oxidation potentials[20] are low enough to reduce each Mn^{III} porphyrin to its Mn^{II} form [Equation (1)]. These reducing agents were prepared by comproportionation of the *p*-benzoquinone derivatives with the corresponding hydroquinone dianions, which were generated by reaction of the hydroquinones with tetra-*n*-butylammonium hydroxide.[21] The rates of electron transfer from the semiquinone radical anion to (TPP)MnCl or (DPPX)MnCl were measured by monitoring the increase in absorbance of the Mn^{II} Soret band {e.g. at 488 nm for $[(DPPH_{20})Mn^{II}Cl]^-$ in Figure 1a} using a stopped-flow technique.

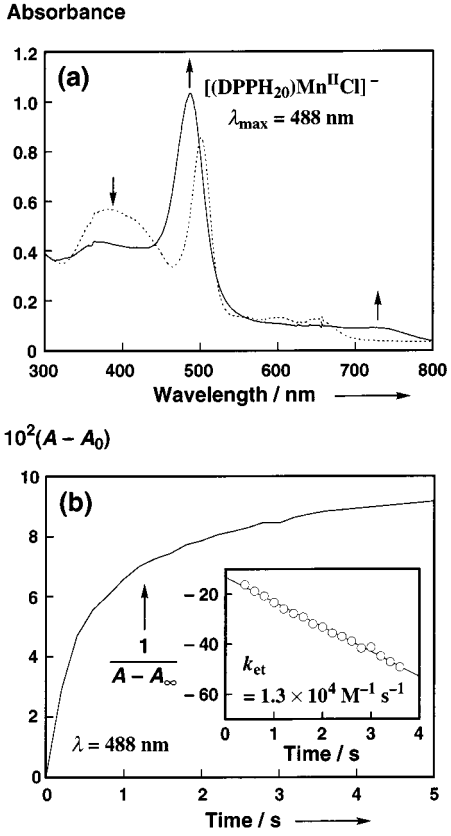

Figure 1. (a) Spectral changes upon addition of $Q^{\bullet -}$ (2.0×10^{-5} M) to a deaerated MeCN solution of $(DPPH_{20})$MnCl (2.0×10^{-5} M) at 298 K; (b) time course of the absorption change at 488 nm in the reaction of $(DPPH_{20})$MnCl (8.3×10^{-5} M) with $Q^{\bullet -}$ (8.3×10^{-5} M) in deaerated MeCN at 298 K; inset: the second-order plot

The electron-transfer rates obey second-order kinetics when the initial concentrations of (P)MnCl and the semiquinone radical anion are equal (Figure 1b). The observed second-order rate constants k_{et} of the electron-transfer reactions are listed in Table 1, which also lists the free-energy change of electron transfer from the semiquinone radical anion to (P)MnCl (ΔG^0_{et}). The ΔG^0_{et} values were calculated from the one-electron reduction potentials of (P)MnCl (E^0_{red}) and the one-electron oxidation potentials of the semiquinone radical anions (E^0_{ox}), which are equivalent to the one-electron reduction potentials of the corresponding quinones[20] by Equation (2), where F is the Faraday constant.

$$\Delta G^0_{et} = F(E^0_{ox} - E^0_{red}) \quad (2)$$

It was confirmed that the k_{et} value for electron transfer from the semiquinone radical anion ($Q^{\bullet-}$) to $(DPPF_{20})MnCl$ in the presence of 0.1 M tetrabutylammonium chloride (1.8×10^5 $M^{-1}\cdot s^{-1}$) is essentially the same as the k_{et} value in the absence of excess Cl^- (2.0×10^5 $M^{-1}\cdot s^{-1}$). This indicates that no dissociation of Cl^- is involved in the electron-transfer reduction of $(DPPF_{20})MnCl$.

The self-exchange rate constants (k_{ex}) of (P)MnCl/[(P)MnCl]$^-$ can be determined from k_{et} and the self-exchange rate constants (k_{ex}') of $Q^{\bullet-}$/Q by using the Marcus equations [Equation (3) and Equation (4)],[22] where K_{et} is the equilibrium constant for electron transfer, f is a correction factor (generally close to 1), and Z is the collision frequency, taken as 1×10^{11} $M^{-1}\cdot s^{-1}$. The self-exchange rate constants (k_{ex}') of $Q^{\bullet-}$/Q was previously determined as 8.1×10^7 $M^{-1}\cdot s^{-1}$ from the linewidth variation of the EPR spectrum of semiquinone radical anion ($Q^{\bullet-}$) in the presence of various concentrations of *p*-benzoquinone (Q) in PhCN at 298 K.[23] The K_{et} values are obtained from the ΔG^0_{et} values by using Equation (5). The k_{ex} values of (P)MnCl/[(P)MnCl]$^-$ thus obtained are listed in Table 1.

$$k_{ex} = k^2_{et}/(k_{ex}' K_{et} f) \quad (3)$$

$$\ln f = (\ln K_{et})^2/4[\ln(k_{ex}\, k_{ex}'/Z^2)] \quad (4)$$

$$K_{et} = \exp(-\Delta G^0_{et}/RT) \quad (5)$$

The k_{ex} values depend significantly on the type of porphyrin macrocycle and decrease in the order: (TPP)MnCl (3.1×10^3 $M^{-1}\cdot s^{-1}$) > $(DPPH_{20})MnCl$ (1.1×10^{-2} $M^{-1}\cdot s^{-1}$) > $(DPPCl_{12}H_8)MnCl$ (3.5×10^{-4} $M^{-1}\cdot s^{-1}$) > $(DPPF_{20})MnCl$ (4.3×10^{-6} $M^{-1}\cdot s^{-1}$). Hence, the electron-transfer rate at a given free energy change of electron transfer should also decrease in this order. This is clearly shown as the plots of lg k_{et} values vs. ΔG^0_{et} in Figure 2, which includes the data for other semiquinone radical anions used as reductants. The dependence of lg k_{et} on ΔG^0_{et} is given by Equation (6) which is derived from Equations 3−5.[22] The reorganization energy of electron transfer (λ) corresponds to the average of each component, λ_{11} for the electron self-exchange of Q/$Q^{\bullet-}$ and λ_{22} of (P)MnCl/[(P)MnCl]$^-$ [Equation (7)]. The fit of the curves to the Marcus theory of adiabatic outer-sphere electron transfer [Equation (6) and Equation (7)][22] indicates that the rate variations at a given ΔG^0_{et} value arise from the difference in the λ value given in Figure 2 and not from the nonadiabaticity.

$$\Delta G^{\ddagger} = (\lambda/4)(1 + \Delta G^0_{et}/\lambda)^2 \quad (6)$$

$$\lambda = (\lambda_{11} + \lambda_{22})/2 \quad (7)$$

The significantly small k_{ex} value of $(DPPF_{20})MnCl$ (4.3×10^{-6} $M^{-1}\cdot s^{-1}$) as compared with that of (TPP)MnCl (3.1×10^3 $M^{-1}\cdot s^{-1}$) may be related to differences in the conformation of the porphyrin macrocycles. The crystal structure of $(DPPF_{20})MnCl$ reveals a nonplanar conformation of the macrocycle because of peripheral congestion of the porphyrin.[16] The Mn^{III} center is located inside the curved

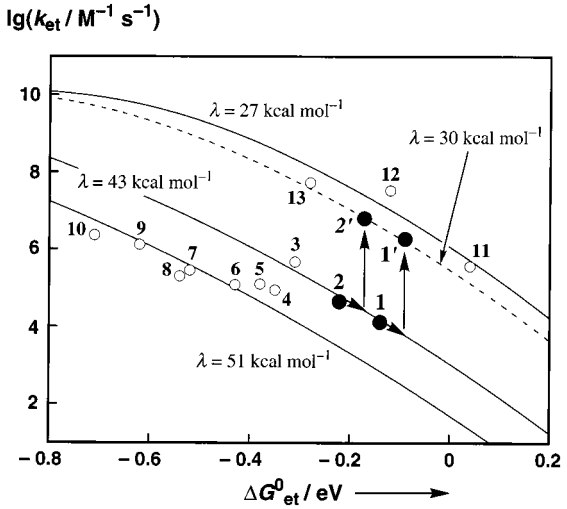

Figure 2. Dependence of lg k_{et} on ΔG^0_{et} for the electron-transfer reductions of the (P)MnCl derivatives by semiquinone radical anions in deaerated MeCN at 298 K; the numbers refer to the system: **1**: $(DPPH_{20})MnCl/Q^{\bullet-}$; **1′**: $[(DPPH_{20})Mn(py)_2]^+/Q^{\bullet-}$; **2**: $(DPPH_{20})MnCl/MeQ^{\bullet-}$; **2′**: $[(DPPH_{20})Mn(py)_2]^+/MeQ^{\bullet-}$; **3**: $(DPPH_{20})MnCl/2,6\text{-}Me_2Q^{\bullet-}$; **4**: $(DPPCl_{12}H_8)MnCl/Q^{\bullet-}$; **5**: $(DPPF_{20})MnCl/ClQ^{\bullet-}$; **6**: $(DPPCl_{12}H_8)MnCl/MeQ^{\bullet-}$; **7**: $(DPPCl_{12}H_8)MnCl/2,6\text{-}Me_2Q^{\bullet-}$; **8**: $(DPPF_{20})MnCl/Q^{\bullet-}$; **9**: $(DPPF_{20})MnCl/Q^{\bullet-}$; **10**: $(DPPF_{20})MnCl/Q^{\bullet-}$; **11**: (TPP)MnCl/2,5-$Cl_2Q^{\bullet-}$; **12**: (TPP)MnCl/$ClQ^{\bullet-}$; **13**: (TPP)MnCl/$Q^{\bullet-}$; 2,6-$Me_2Q$ = 2,6-dimethyl-*p*-benzoquinone, MeQ = methyl-*p*-benzoquinone, Q = *p*-benzoquinone, ClQ = chloro-*p*-benzoquinone, 2,5-Cl_2Q = 2,5-dichloro-*p*-benzoquinone; the solid and dashed lines are drawn based on the Marcus theory of electron transfer [Equation (6)and Equation (7)] using the λ values shown in the figure (see text)

surface of the nonplanar porphyrin macrocycle with a Mn^{III}−N distance of 1.99(1) Å.[16a] The strong binding of Mn^{III} to the nonplanar porphyrin causes a major bond-reorganization on the reduction of Mn^{III} to Mn^{II} and this is accompanied by a metal out-of-plane displacement since an electron is added to the $d_{x^2-y^2}$ orbital which directly interacts with the pyrrole nitrogen orbitals. Hence, the greater the nonplanarity of the porphyrin ligand, the stronger seems to be the binding of Mn^{III} to the ligand, the larger is the reorganization energy of the electron-transfer reduction and the smaller is the k_{ex} value, as was experimentally observed in the present study.

Effects of Axial Coordination on Electron Transfer

The slow electron-transfer reduction of nonplanar manganese porphyrins can be accelerated by axial coordination of a base since the addition of a nitrogenous base such as pyridine (py) to five-coordinate metalloporphyrins often results in substantial changes in the redox reactivities.[1,2,24,25] The addition of pyridine to an MeCN solution of $(DPPH_{20})MnCl$ results in a significant change in the UV/vis spectrum, as shown in Figure 3.

These changes can be analyzed by Equation (8), which is derived by assuming that *n* molecules of pyridine coordinate to $(DPPH_{20})MnCl$.

$$\lg[(A_0 - A)/(A - A_\infty)] = n\lg[py] + \lg K \quad (8)$$

In this Equation A_0 is the absorbance of $(DPPH_{20})MnCl$ in the absence of pyridine, A_∞ is the absorbance of the fully

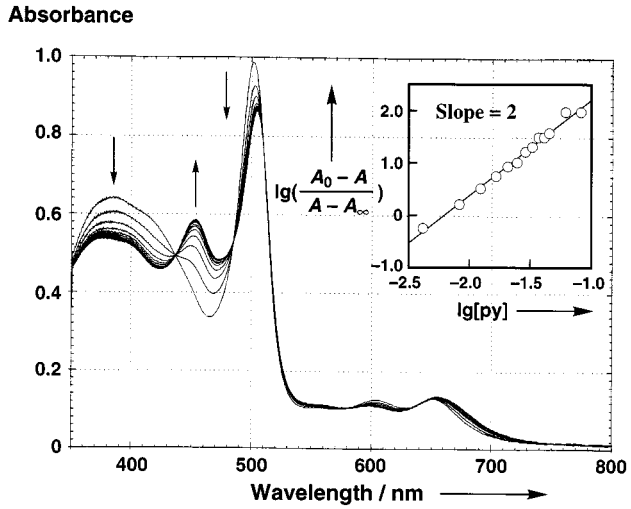

Figure 3. Spectral changes upon addition of py (4.1×10^{-3} M, each) to a deaerated MeCN solution of $(DPPH_{20})Mn^{III}Cl$ (1.8×10^{-5} M) at 298 K; inset: plot of $\lg[(A_0 - A)/(A - A_\infty)]$ vs. lg[py]; A_0, A, A_∞: absorbance at 452 nm

formed complex with pyridine, A is the absorbance of the equilibrium mixture, and K is the formation constant. The slope, n, in such plot gives the number of molecules of pyridine coordinated. The plot of $\lg[(A_0 - A)/(A - A_\infty)]$ vs. lg[py] (inset in Figure 3) indicates that two molecules of pyridine coordinate to $(DPPH_{20})MnCl$ to form the six coordinate complex $[(DPPH_{20})Mn(py)_2]^+$ (λ_{max} = 477 nm) and a lg$K$ value of 4.0 is calculated under the given experimental conditions [Equation (9)].

$$(DPPH_{20})Mn^{III}Cl + 2py \overset{K}{\rightleftharpoons} [(DPPH_{20})Mn^{III}(py)_2]Cl \quad (9)$$

The addition of pyridine to the $(DPPH_{20})MnCl$/reductant system results in a significant increase in the rate of electron transfer from the reductant to $(DPPH_{20})MnCl$. Most electron-transfer rates of (DPPX)MnCl in the presence of pyridine were so rapid so as to fall outside the stopped-flow range. Thus, the least reactive systems in Table 1, i.e. the $(DPPH_{20})MnCl/Q^{\bullet-}$ and $(DPPH_{20})MnCl/MeQ^{\bullet-}$ systems were chosen to determine the effect of pyridine on the electron-transfer rate. The electron-transfer rate constant k_{et} increases with an increase in the pyridine concentration to reach a constant value as shown in Figure 4.

The acceleration of the rate of electron transfer by the binding of pyridine may be ascribed to the much faster electron-transfer rate-constant for the six-coordinate complex ($k_{et(6)}$), $[(DPPH_{20})Mn(py)_2]^+$, than that for the five-coordinate complex ($k_{et(5)}$), $(DPPH_{20})MnCl$, as shown in Scheme 1. The $k_{et(6)}$ value for electron transfer from $Q^{\bullet-}$ to $[(DPPH_{20})Mn(py)_2]^+$ of 1.9×10^6 $M^{-1}\cdot s^{-1}$ was determined from the constant value in Figure 4 and is two orders of magnitude larger than the $k_{et(5)}$ value (1.3×10^4 $M^{-1}\cdot s^{-1}$) as shown in Table 1. Similarly, the $k_{et(6)}$ value for electron transfer from $MeQ^{\bullet-}$ to $[(DPPH_{20})Mn(py)_2]^+$ was determined from the data in Figure 4 to be 5.8×10^6 $M^{-1}\cdot s^{-1}$, which is also two orders of magnitude larger than the $k_{et(5)}$ value (4.1×10^4 $M^{-1}\cdot s^{-1}$).

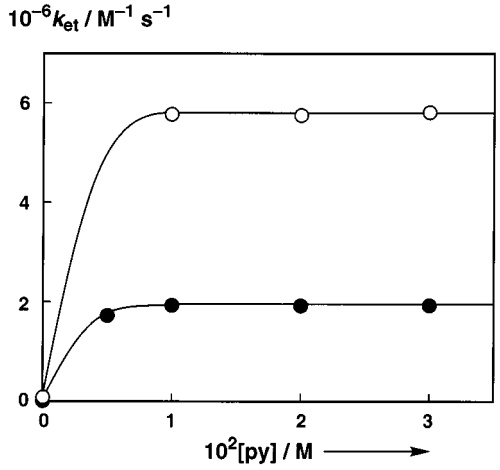

Figure 4. Plot of k_{et} vs. [py] for the electron transfer from $Q^{\bullet-}$ (filled circles; 9.1×10^{-6} M) or $MeQ^{\bullet-}$ (open circles; 9.1×10^{-6} M) to $(DPPH_{20})MnCl$ (9.1×10^{-6} M) in the presence of py in deaerated MeCN at 298 K

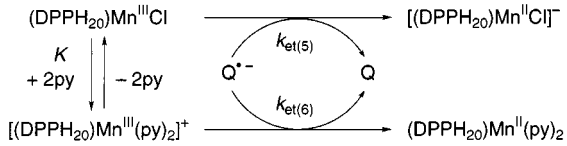

Scheme 1. Base-catalyzed electron transfer

The one-electron reduction potential might be expected to shift in a negative direction by the axial ligand coordination of pyridine when the electron-transfer reduction becomes energetically less favorable. However, the reduction of $[(DPPH_{20})Mn(py)_2]^+$ occurs at $E^0_{red} = -0.41$ V vs. SCE which is only slightly more negative than the E^0_{red} value (−0.36 V) of the five-coordinate complex $(DPPH_{20})MnCl$ (Table 1). Such a small negative shift of the reduction potential by coordination of pyridine cannot account for the large acceleration in the rate of electron transfer for the six-coordinate complex as compared to the five coordinate complex, as shown by the arrows along the curve with a constant λ value in Figure 2. Thus, the acceleration in the rate of electron transfer upon axial coordination of pyridine results from a significant decrease in the reorganization energy associated with the electron-transfer reduction of $[(DPPH_{20})Mn(py)_2]^+$. This is shown by the vertical arrows in Figure 2 where the dependence of k_{et} for the electron-transfer reduction of $[(DPPH_{20})Mn(py)_2]^+$, using a λ value of 30 kcal mol^{-1}, is given by the dashed line. The λ value becomes close to the value for the planar porphyrin (27 $kcal\cdot mol^{-1}$ for TPPMnCl). The acceleration effect of pyridine on the rates of electron transfer for the other (DPPX)MnCl complexes could not be determined quantitatively because of the fast electron-transfer rates for $[(DPPX)Mn(py)_2]^+$ which are beyond the detection limit of a stopped-flow technique, but such a rate-acceleration effect of pyridine indicates a significant decrease in the reorganization energy upon the axial ligand-coordination of the base. The k_{ex} values of $[(DPPH_{20})Mn(py)_2]^+$ (1.5×10^3 $M^{-1}\cdot s^{-1}$) determined from the k_{et} value using Equation (3)

and Equation (4) is five orders of magnitude larger than that of $(DPPH_{20})MnCl$ (Table 1).

We have also examined the rates of electron-transfer reduction of $(DPPH_{20})MnCl$ by $Q^{\bullet-}$ in deaerated DMSO. The UV/vis spectrum of the Mn^{III} complex in DMSO is similar to that in pyridine, suggesting that the six-coordinate complex $[(DPPH_{20})Mn(DMSO)_2]^+$ (λ_{max} = 480 nm) is formed in DMSO. The rate of electron-transfer from $Q^{\bullet-}$ to the Mn^{III} complex in DMSO was determined to be 2.3×10^6 $M^{-1}\cdot s^{-1}$, which is essentially the same as that of $[(DPPH_{20})Mn(py)_2]^+$ (1.9×10^6 $M^{-1}\cdot s^{-1}$). Addition of one mol of pyridine to a deaerated DMSO solution of Mn^{III} complex resulted in little acceleration of the electron-transfer reduction of the Mn^{III} complex by $Q^{\bullet-}$ (2.7×10^6 $M^{-1}\cdot s^{-1}$). These results indicate that the rates of electron-transfer reduction of the six-coordinate Mn^{III} porphyrins are much faster than those of the five-coordinate Mn^{III} porphyrins because of the smaller reorganization energies in the six-coordinate complex upon electron transfer than the five-coordinate complex, as observed in the case of the electron-transfer oxidation of (OETPP)Fe(R).[2]

Experimental Section

Materials: The synthesis and characterization of (P)MnCl (P = TPP or DPPX where X = H_{20}, $C_{12}H_8$ or F_{20}) have been reported in the literature.[16,19] *p*-Benzoquinone derivatives (2,6-Me_2Q: 2,6-dimethyl-*p*-benzoquinone; MeQ: methyl-*p*-benzoquinone; Q: *p*-benzoquinone; ClQ: chloro-*p*-benzoquinone; 2,5-Cl_2Q: 2,5-dichloro-*p*-benzoquinone) as well as the corresponding hydroquinones were purchased from Tokyo Chemical Industry Co., Ltd., and recrystallized from ethanol prior to use. Tetra-*n*-butylammonium hydroxide (TBAOH: 1.0 M in methanol) was purchased from Aldrich and used as received. Acetonitrile (MeCN) and benzonitrile (PhCN) were purchased from Wako Pure Chemical Ind. Ltd., and purified by successive distillation over CaH_2 and P_2O_5 according to standard procedures.[26] Tetra-*n*-butylammonium perchlorate (TBAP) was purchased from Sigma Chemical Co., recrystallized from ethanol, and dried under vacuum at 40 °C prior to use.

Spectral and Kinetic Measurements: Typically, a 3.0 μL aliquot of semiquinone radical anion ($Q^{\bullet-}$: 0.02 M) in MeCN was prepared by comproportionation between *p*-benzoquinone (Q: 0.01 M) and hydroquinone (QH_2: 0.01 M) in the presence of 0.02 M TBAOH[21] and then added to a quartz cuvette (10 mm i.d.) which contained $(DPPH_{20})MnCl$ (2.0×10^{-5} M) in deaerated MeCN (3.0 mL). This led to an electron transfer from $Q^{\bullet-}$ to $(DPPH_{20})MnCl$. The UV/visible spectral changes associated with this electron transfer were monitored with the use of a Hewlett Packard 8453 diode array spectrophotometer. The same procedure was used to follow reactions of other manganese porphyrins. The binding of pyridine or DMSO to $(DPPH_{20})MnCl$ in MeCN was monitored by measuring the UV/vis spectral changes as a function of the ligand concentration. All measurements were carried out in a dark cell compartment using deaerated conditions. It was confirmed that the monitoring light did not affect the thermal rates.

Kinetic measurements for electron transfer from $Q^{\bullet-}$ to (P)MnCl were carried out using a Union RA-103 stopped-flow spectrophotometer under deaerated conditions. Typically, deaerated MeCN solutions of (P)MnCl and $Q^{\bullet-}$ were transferred to the spectrophotometric cell by means of a glass syringe which had earlier been purged with a stream of argon. The rates of the electron transfer (k_{et}) were followed by monitoring an increase in the absorbance due to the reduced porphyrin product, $[(P)MnCl]^-$ (e.g. at 488 nm for $[(DPPH_{20})MnCl]^-$), under second-order conditions where the initial concentrations of (P)MnCl and $Q^{\bullet-}$ are the same. In each case, it was confirmed that the k_{et} values derived from at least five independent measurements which agreed within an experimental error of ±5%. Second-order rate constants were determined by a least-squares curve fit using a Macintosh personal computer. The second-order plots of $(A_\infty - A)^{-1}$ vs. time (A_∞ and A are the final absorbance and the absorbance at the reaction time, respectively) were linear for three or more half-lives with the correlation coefficient, $\rho > 0.999$.

Cyclic Voltammetry: The redox potentials of (P)MnCl in PhCN or MeCN containing 0.1 M TBAP as supporting electrolyte were determined at room temperature by cyclic voltammetry under deaerated conditions using a three electrode system and a BAS 100B electrochemical analyzer. The working and counter electrodes were platinum while $Ag/AgNO_3$ (0.01 M) was used as the reference electrode. All potentials are reported as V vs. SCE. The $E_{1/2}$ value of ferrocene used as a standard is approximately 0.37 V vs. SCE in PhCN or MeCN under our solution conditions.[27]

Acknowledgments

This work was partially supported by an International Scientific Research Program (No. 11694079) and a Grant-in-Aid for Scientific Research Priority Area (Nos. 11133232 and 11136229) from the Ministry of Education, Science, Culture and Sports, Japan. R. G. acknowledges support from the CNRS. K. M. K. also acknowledges support from the Robert A. Welch Foundation (Grant E-680).

[1] S. Fukuzumi, *The Porphyrin Handbook* (Eds.: K. M. Kadish, K. M. Smith, R. Guilard), Academic Press, San Diego, CA, **1999**, Vol. 8, 115−151.
[2] S. Fukuzumi, I. Nakanishi, K. Tanaka, T. Suenobu, A. Tabard, R. Guilard, E. Van Caemelbecke, K. M. Kadish, *J. Am. Chem. Soc.* **1999**, *121*, 785−790.
[3] W. R. Scheidt, Y. J. Lee, *Struc. Bonding (Berlin)* **1987**, *64*, 1−70.
[4] [4a] H.-C. Chow, R. Serlin, C. E. Strouse, *J. Am. Chem. Soc.* **1975**, *97*, 7230−7237. − [4b] R. Serlin, H.-C. Chow, C. E. Strouse, *J. Am. Chem. Soc.* **1975**, *97*, 7237−7242.
[5] [5a] S. Gentemann, C. J. Medforth, T. P. Forsyth, D. J. Nurco, K. M. Smith, J. Fajer, D. Holten, *J. Am. Chem. Soc*. **1994**, *116*, 7363−7368. − [5b] K. M. Barkigia, M. D. Berber, J. Fajer, C. J. Medforth, M. W. Renner, K. M. Smith, *J. Am. Chem. Soc.* **1990**, *112*, 8851−8857.
[6] T. L. Horning, E. Fujita, J. Fajer, *J. Am. Chem. Soc*. **1986**, *108*, 323−325.
[7] R. G. Alden, M. R. Ondrias, J. A. Shelnutt, *J. Am. Chem. Soc*. **1990**, *112*, 691−697.
[8] K. M. Barkigia, L. Chantranupong, K. M. Smith, J. Fajer, *J. Am. Chem. Soc*. **1988**, *110*, 7566−7567.
[9] J. A. Shelnutt, C. J. Medforth, M. D. Berber, K. M. Barkigia, K. M. Smith, *J. Am. Chem. Soc.* **1991**, *113*, 4077−4087.
[10] J. Takeda, T. Ohya, M. Sato, *Inorg. Chem*. **1992**, *31*, 2877−2880.
[11] C. J. Medforth, J. D. Hobbs, M. R. Rodriguez, R. J. Abraham, K. M. Smith, J. A. Shelnutt, *Inorg Chem*. **1995**, *34*, 1333−1341.
[12] [12a] K. M. Faulkner, S. I. Liochev, I. Fridovich, *J. Biol. Chem.* **1994**, *269*, 23471−23476. − [12b] P. R. Gardner, D. D. H. Nguyen, C. W. White, *Arch. Biochem. Biophys.* **1996**, *325*, 20−28. − [12c] M. Hoshino, Y. Nagashima, H. Seki, M. De Leo, P. C. Ford, *Inorg. Chem.* **1998**, *37*, 2464−2469.
[13] B. Meunier, *Chem. Rev.* **1992**, *92*, 1411−1456.

[14] [14a] L. O. Spreer, A. C. Maliyackel, S. Holbrook, J. W. Otvos, M. Calvin, *J. Am. Chem. Soc.* **1986**, *108*, 1949−1953. − [14b] A. C. Maliyackel, J. W. Otvos, M. Calvin, L. O. Spreer, *Inorg. Chem.* **1987**, *26*, 4133−4135. − [14c] M. Schappacher, R. Weiss, *Inorg. Chem.* **1987**, *26*, 1189−1190. − [14d] R. S. Czernuszewicz, Y. O. Su, M. K. Stern, K. A. Macor, D. Kim, J. T. Groves, T. G. Spiro, *J. Am. Chem. Soc.* **1988**, *110*, 4158−4165. − [14e] K. R. Rodgers, H. M. Goff, *J. Am. Chem. Soc.* **1988**, *110*, 7049−7060. − [14f] J. T. Groves, M. K. Stern, *J. Am. Chem. Soc.* **1988**, *110*, 8628−8638. − [14g] R. D. Arasasingham, T. C. Bruice, *Inorg. Chem*. **1990**, *29*, 1422−1427. − [14h] R. J. Balahura, R. A. Kirby, *Inorg. Chem.* **1994**, *33*, 1021−1025.

[15] K. M. Kadish, M. Sweetland, J. S. Cheng, *Inorg. Chem*. **1978**, *17*, 2795−2797.

[16] [16a] R. Guilard, K. Perié, J.-M. Barbe, D. J. Nurco, K. M. Smith, E. Van Caemelbecke, K. M. Kadish, *Inorg. Chem.* **1998**, *37*, 973−981. − [16b] K. Perie, J. M. Barbe, P. Cocolios, R. Guilard, *Bull. Soc. Chim. Fr.* **1996**, *133*, 697−702.

[17] [17a] X. H. Mu, F. A. Schultz, *Inorg. Chem.* **1992**, *31*, 3351−3357. − [17b] X. H. Mu, F. A. Schultz, *J. Electroanal. Chem.* **1993**, *353*, 349−355. − [17c] D. Feng, F. A. Schultz, *Inorg. Chem.* **1988**, *27*, 2144−2149. − [17d] X. H. Mu, F. A. Schultz, *Inorg. Chem.* **1990**, *29*, 2877−2879.

[18] K. M. Kadish, D. G. Davis, *Ann. N. Y. Acad. Sci.* **1973**, *206*, 495−503.

[19] S. Fukuzumi, I. Nakanishi, J.-M. Barbe, R. Guilard, E. Van Caemelbecke, N. Guo, K. M. Kadish, *Angew. Chem.* **1999**, *111*, 1017−1019; *Angew. Chem. Int. Ed.* **1999**, *38*, 964−966.

[20] S. Fukuzumi, S. Koumitsu, K. Hironaka, T. Tanaka, *J. Am. Chem. Soc.* **1987**, *109*, 305−316.

[21] S. Fukuzumi, T. Yorisue, *Bull. Chem. Soc. Jpn.* 1992, *65*, 715−719.

[22] [22a] R. A. Marcus, *Annu. Rev. Phys. Chem.* **1964**, *15*, 155−196. − [22b] R. A. Marcus, *Angew. Chem.* **1993**, *105*, 1161−1172; *Angew. Chem. Int. Ed. Engl.* **1993**, *32*, 1111−1121.

[23] ESR linewidth analysis: [23a] R. Chang, *J. Chem. Educ.* **1970**, *47*, 563−568. − [23b] K. S. Cheng, N. Hirota, *Investigation of Rates and Mechanisms of Reaction, Vol. VI* (Ed.: G. G. Hammes), Wiley, New York, **1974**, 565−636. − [23c] I. Nakanishi, S. Itoh, T. Suenobu, S. Fukuzumi, *Chem. Commun.* **1997**, 1927−1928. − [23d] S. Fukuzumi, I. Nakanishi, T. Suenobu, K. M. Kadish, *J. Am. Chem. Soc.* **1999**, *121*, 3468−3474.

[24] [24a] K. M. Kadish, *Iron Porphyrins, Part 2* (Eds.: A. B. P. Lever, H. B. Gray), Addison-Wesley, Reading, MA, **1982**, 161−249. − [24b] K. M. Kadish, L. A. Bottomley, *Inorg. Chem.* **1980**, *19*, 832−836. − [24c] F. A. Walker, J. A. Barry, V. L. Balke, G. A. McDermott, M. Z. Wu, P. F. Linde, *Adv. Chem. Ser.* **1981**, *201*, 377−416.

[25] D. Lançon, P. Cocolios, R. Guilard, K. M. Kadish, *Organometallics* **1984**, *3*, 1164−1170.

[26] D. D. Perrin, W. L. F. Armarego, D. R. Perrin, *Purification of Laboratory Chemicals*; Pergamon Press, Elmsford, NY, **1966**.

[27] C. K. Mann, K. K. Barnes, *Electrochemical Reactions in Nonaqueous Systems*, Marcel Dekker, Inc., New York, **1990**.

Received December 10, 1999
[I99450]